Water-enhanced bifunctional metal-aside catalyst for C=C bond hydrogenation

Shoutian Sun,[1] Gengnan Li,[1,2] Thomas Salas,[1] Daniel E. Resasco,[1] Bin Wang[1,3,4]*

1 School of Sustainable Chemical, Biological and Materials Engineering, University of Oklahoma, Norman, OK 73019, USA

2 Argonne National Laboratory 9700 S. Cass Avenue Lemont, IL 60439

3 Department of Chemical and Biological Engineering, Tufts University, Medford, MA 02155, USA

4 Max Planck Institute for Sustainable Materials GmbH, D–40237 Düsseldorf, Germany

Corresponding author: bin.wang@tufts.edu

To support the proposed competitive adsorption mechanism, we calculated the adsorption energies of cyclohexene and water on the metal surface. The adsorption energy for cyclohexene and water is −1.13 and −0.49 eV, respectively. Both values were calculated in vacuum and likely overestimated due to the partial solvation. We constructed a simple competitive Langmuir adsorption model to estimate the surface coverage of both species:

$$\theta_C = \frac{K_C C_C}{1 + K_C C_C + K_W C_W}$$

$$\theta_W = \frac{K_W C_W}{1 + K_C C_C + K_W C_W}$$

K_C and K_W are adsorption equilibrium constants for cyclohexene and water. C_W and C_C are the concentration of the two molecules. Assuming that the hydrogenation step requires both an adsorbed cyclohexene molecule and a nearby water molecule (e.g., to facilitate proton transfer), the rate can be approximated as

$$r \propto \theta_C \theta_W$$

The resulting model naturally reproduces the experimentally observed non-monotonic dependence of the rate on water concentration (Figure S1): at low water content, increasing water enhances the probability of forming cyclohexene–water interfacial pairs and accelerates the reaction, while at higher water concentrations, competitive adsorption of water suppresses cyclohexene adsorption and decreases the rate.

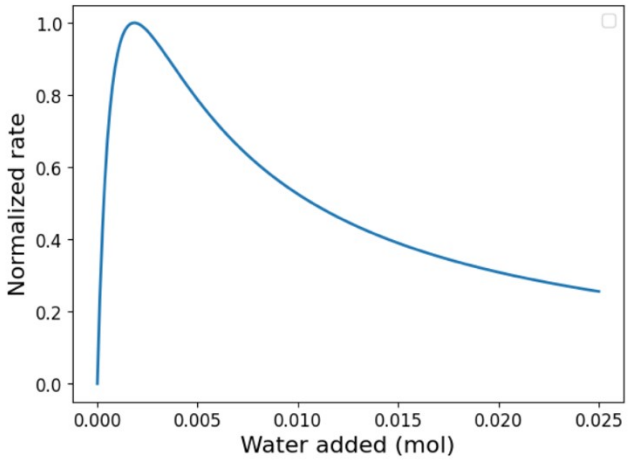

Figure S1. Predicted dependence of the normalized reaction rate on the amount of added water based on a simple Langmuir competitive adsorption model.

The parameters used in the model were chosen based on the experimental reaction conditions. The total liquid volume was taken as V = 0.060 L, corresponding to the

mixture of 1.0 mL cyclohexene and 59 mL dodecane solvent. The cyclohexene concentration was estimated as C_c = 0.164 mol/L. The water concentration was calculated from the added amount of water using $C_w = n_w/V$. Effective adsorption constants of $K_c = 50$ for cyclohexene and $K_w = 300$ for water were used to represent the competitive adsorption behavior under reaction conditions. We used a larger value for water, as in the dodecane solvent, it is anticipated that water is concentrated at the interface due to its low solubility in dodecane and strong interaction with Ni, displacing both cyclohexene and dodecane from the surface. These parameters should be regarded as effective values in a qualitative model rather than exact thermodynamic adsorption constants, and they were selected to reproduce the experimentally observed trend in which the reaction rate reaches a maximum at intermediate water loading.

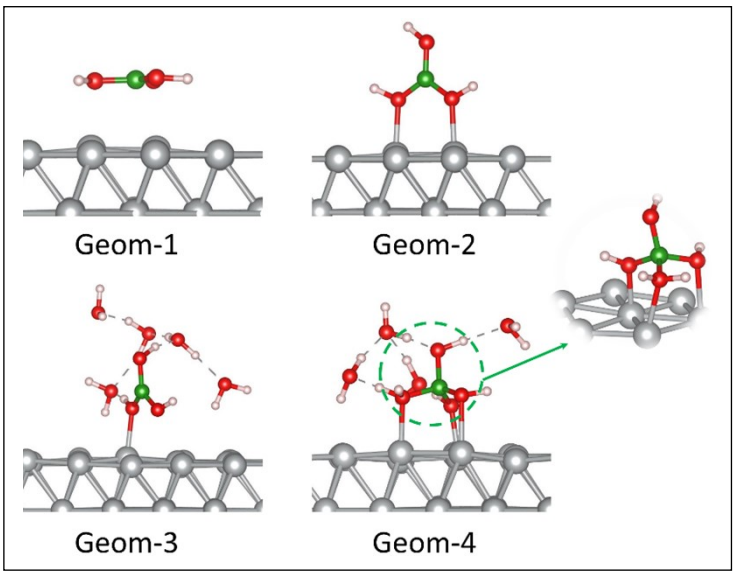

Figure S2. Parallel and vertical adsorption geometries of $B(OH)_3$ on Ni(111) surface (Geom-1 and Geom-2). Water solvated planar-$B(OH)_3$ (Geom-3) and the pyramid H_2O-$B(OH)_3$ complex (Geom-4) on Ni(111) surface at 300 K observed in MTD simulation.

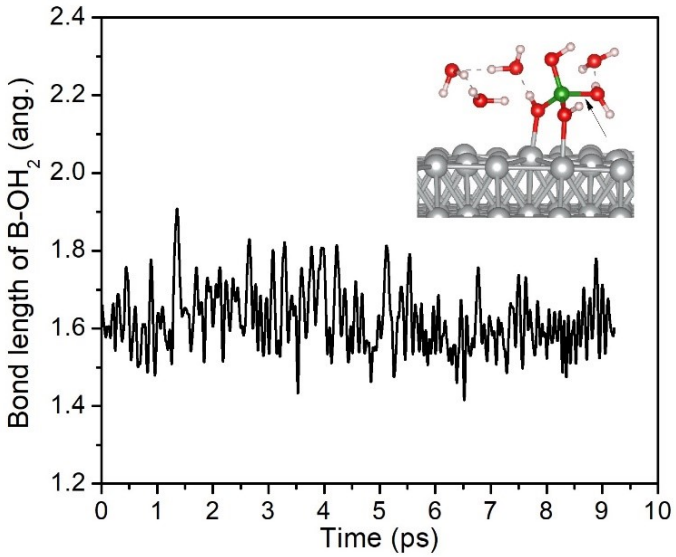

Figure S3. Variation of bond length (B-OH_2, marked with a black arrow) during AIMD simulation of pyramid H_2O-$B(OH)_3$ complex on Ni(111) surface at 300 K.

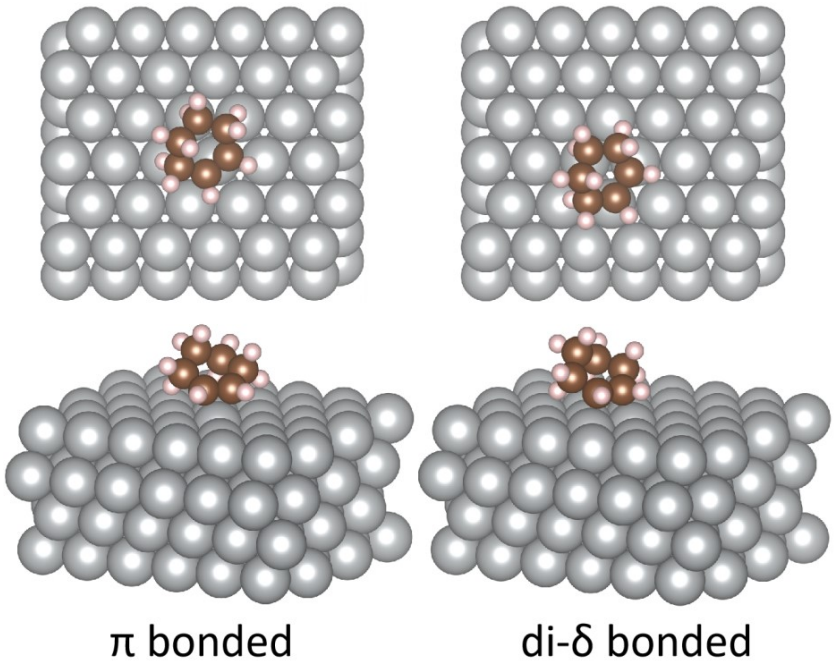

Figure S4. Top and side views of di-δ and π bonded adsorption of cyclohexene (C_6H_{10}) on Ni(111) surface.

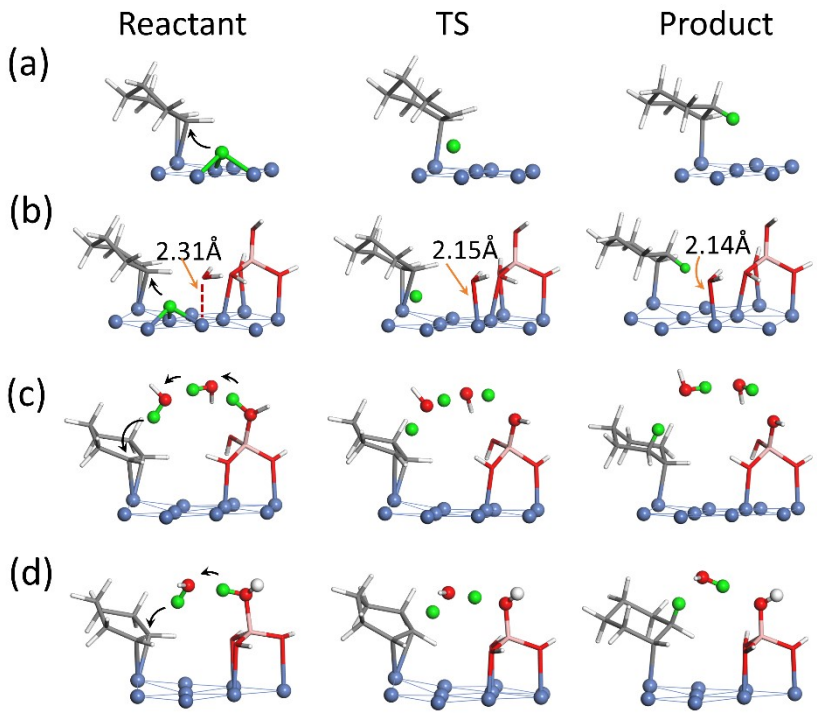

Figure S5. Reactant, transition state (TS), and products for first protonation step: Direct (a), Direct-H_2O (b), H-shuttle-$2H_2O$ (c), and H-shuttle-$1H_2O$ (d), respectively.

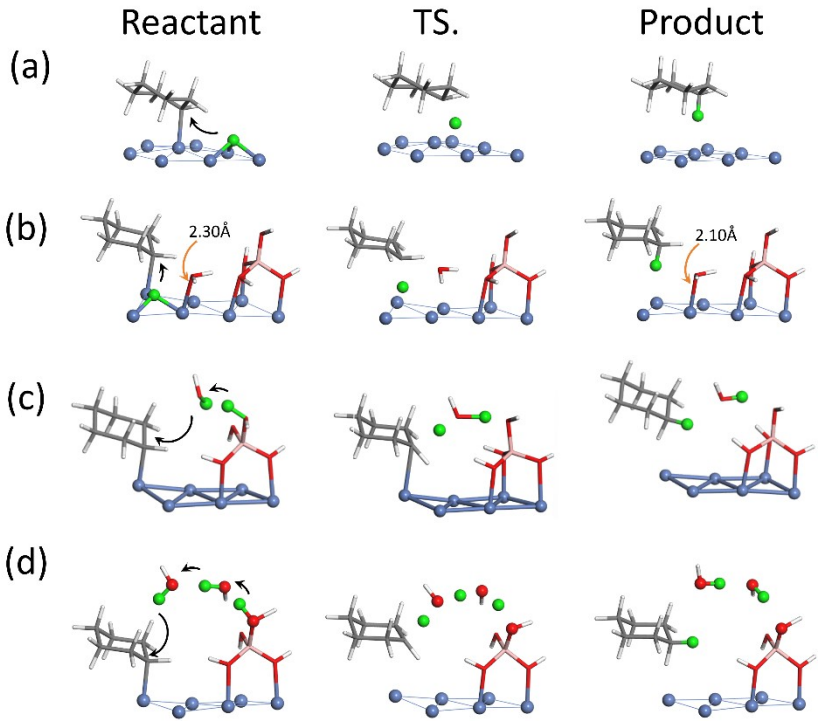

Figure S6. Reactant, TS, and products for second protonation: Direct (a), Direct-H_2O (b), H-shuttle-$1H_2O$ (c), and H-shuttle-$2H_2O$ (d), respectively.

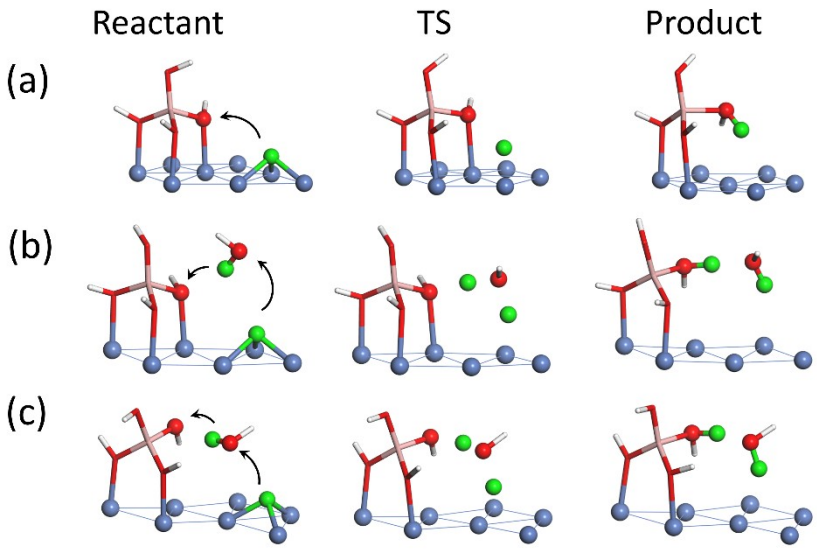

Figure S7. Reactant, TS, and products for second protonation: Direct (a), H-shuttle-1(b), and H-shuttle-2 (c), respectively.

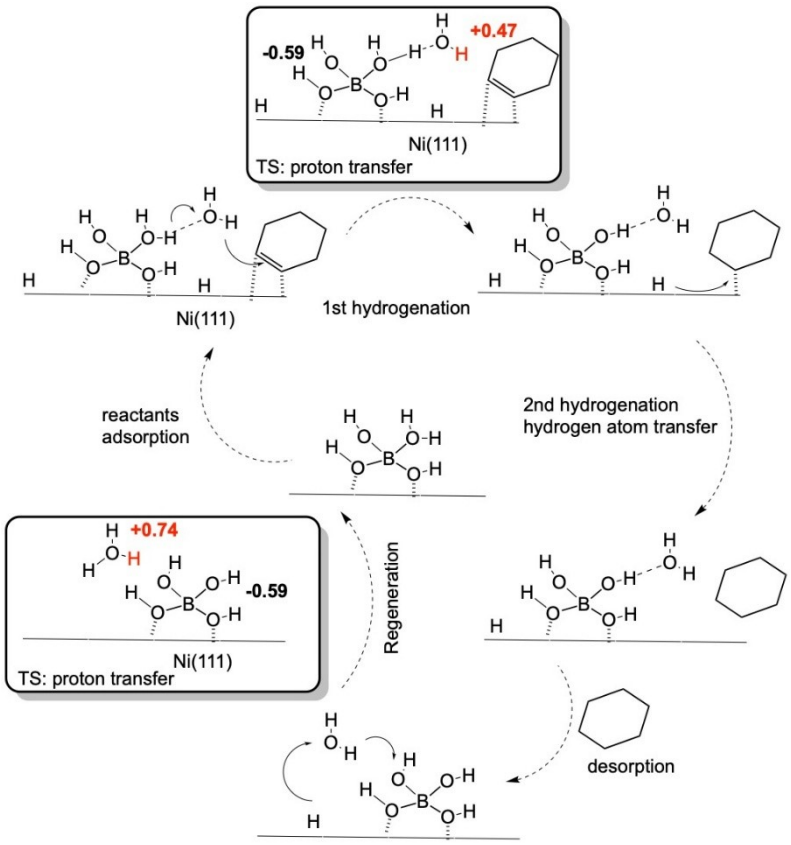

Figure S8. Reaction cycle of H_2O-$B(OH)_3$ complex as catalyst for protonation of C_6H_{10} on Ni(111) surface.

Table S1. Bader charges of transition-state species in the first protonation step of C_6H_{10} for direct H transfer and H-shuttling mechanisms with one or two water molecules.

Unit: |e|	Ni(111)	proton	C_6H_{10}	$B(OH)_4^-+H_2O$
Direct	0.112	-0.113	0.001	-
H-shuttle-1H_2O	0.209	0.467	-0.196	-0.481
H-shuttle-2H_2O	0.329	0.431	-0.222	-0.537

Table S2. Bader charges of initial and transition-state and their charge difference in the second protonation step of C_6H_{10} for direct H transfer. The charge unit is |e|.

	Ni(111)	H	C_6H_{11}
Init.	0.32	-0.23	-0.08
TS.	0.04	-0.04	0.00
Diff.	-0.28	0.20	0.08

Table S3. Bader charges of transition-state species in the second protonation step of C_6H_{10} for direct H transfer with or without adjacent $B(OH)_4^-+H_2O$ species.

Unit: |e|	Ni(111)	proton	C_6H_{11}	$B(OH)_4^-$ +H_2O
Without	0.04	-0.04	0.00	-
With	0.56	0.04	-0.03	-0.57